

Supplement

Rad51 paralogs Rad55-Rad57 balance the anti-recombinase Srs2 in Rad51 filament formation

Jie Liu¹, Ludovic Renault², Xavier Veaute³, Francis Fabre³, Henning Stahlberg^{2,4}, and Wolf-Dietrich Heyer^{1,2,#}

¹ Department of Microbiology and ² Department of Molecular & Cellular Biology, University of California at Davis, Davis, CA95616-8665, USA

³ CEA–DSV-Institut de Radiobiologie Cellulaire et Moléculaire, UMR217 CNRS/CEA, F-92265 Fontenay aux Roses, France

⁴ Center for Cellular Imaging and Nanoanalytics, University Basel, CH-4056 Basel, Switzerland

Corresponding author:

Wolf-Dietrich Heyer Tel. (530) 752-3001, FAX (530) 752-3011. Email wdheyer@ucdavis.edu

Supplementary Table 1: Distribution of Rad55-Rad57 in Rad51 filaments observed by immunoaffinity gold labeling.

	Filament number	Gold particles Terminally	Gold particles interstitially	% filaments associated with gold particle
Rad51-Rad55- Rad57	83	40	43	90
Rad51 only filament	127	0	6	4.7
Rad51 only filament + GST	111	6	3	8.1

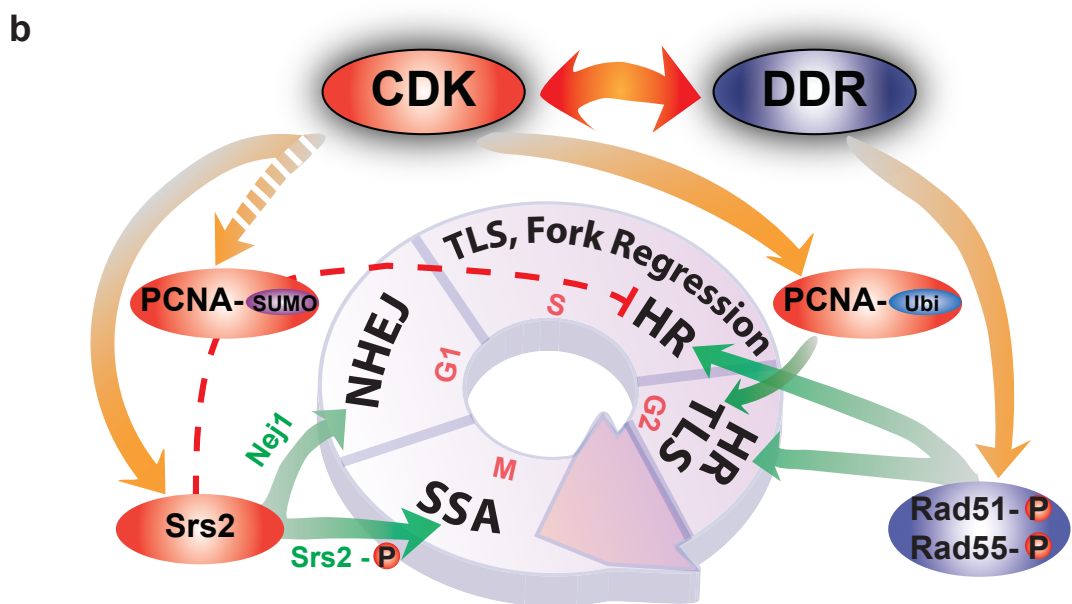
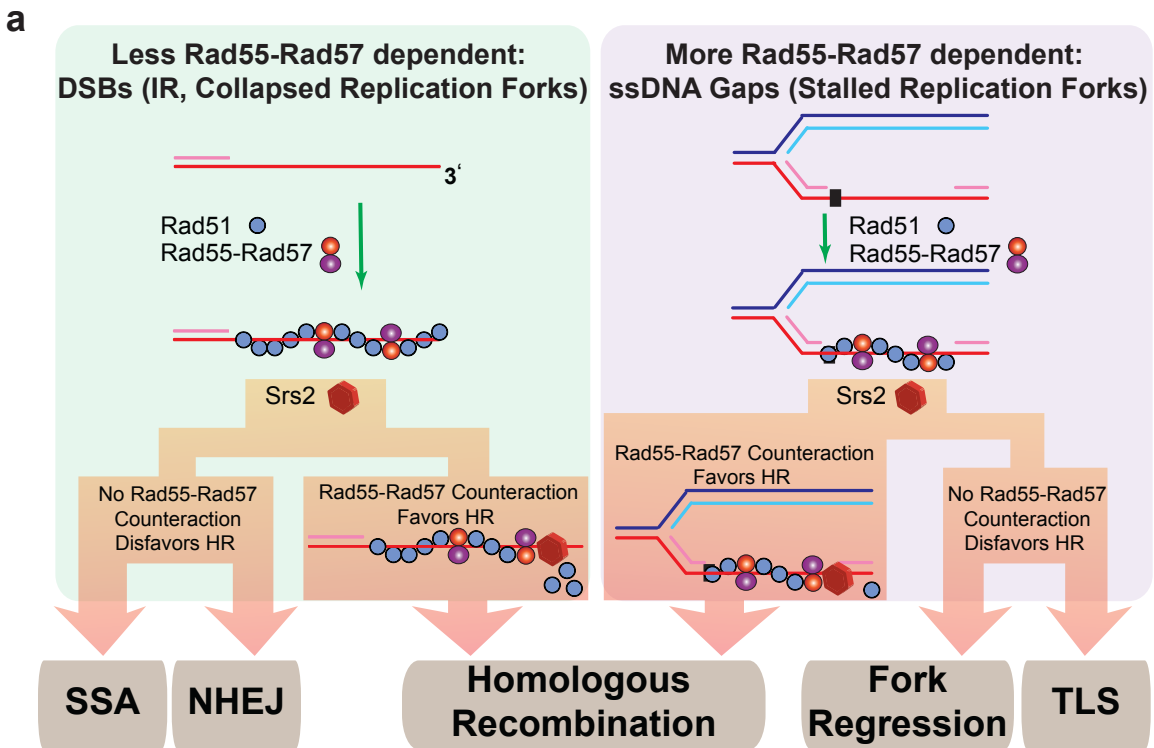
The location of Rad55 in the filaments was analyzed by immuno-gold labeling of GST-Rad55 (see Fig. 1c, d). Rad51 only filaments and Rad51 filaments in the presence of GST serve as negative controls for non-specific labeling by gold particles.

Supplementary Table 2. *Saccharomyces cerevisiae* strains used in this study.

Strain	Genotype
FF18733 ^a	Wild type
FF181461 ^a	<i>rad55Δ::KanMX</i>
WDHY1163 ^a	<i>rad57Δ::URA3^{KI}</i>
FF18744 ^a	<i>srs2Δ::LEU2</i>
FF181464 ^a	<i>rad55Δ::KanMX srs2Δ::LEU2</i>
FF181477 ^a	<i>rad57Δ::URA3^{KI} srs2Δ::LEU2</i>
WDHY1636 ^b	Wild type
WDHY2009 ^b	<i>rad55Δ::URA3^{KI}</i>
WDHY2388 ^b	<i>sml1Δ::HIS3 srs2Δ::KanMX</i>
WDHY2608 ^b	<i>sml1Δ::HIS3 srs2Δ::KanMX rad55Δ::URA3^{KI}</i>
WDHY2319 ^b	<i>ade2-n-URA3-ade2-a</i>
WDHY2019 ^b	<i>rad55Δ::LEU2 ade2-n-URA3-ade2-a</i>
WDHY2632 ^b	<i>srs2Δ::KanMX ade2-n-URA3-ade2-a</i>
WDHY2629 ^b	<i>rad55Δ::LEU2 srs2Δ::KanMX ade2-n-URA3-ade2-a</i>

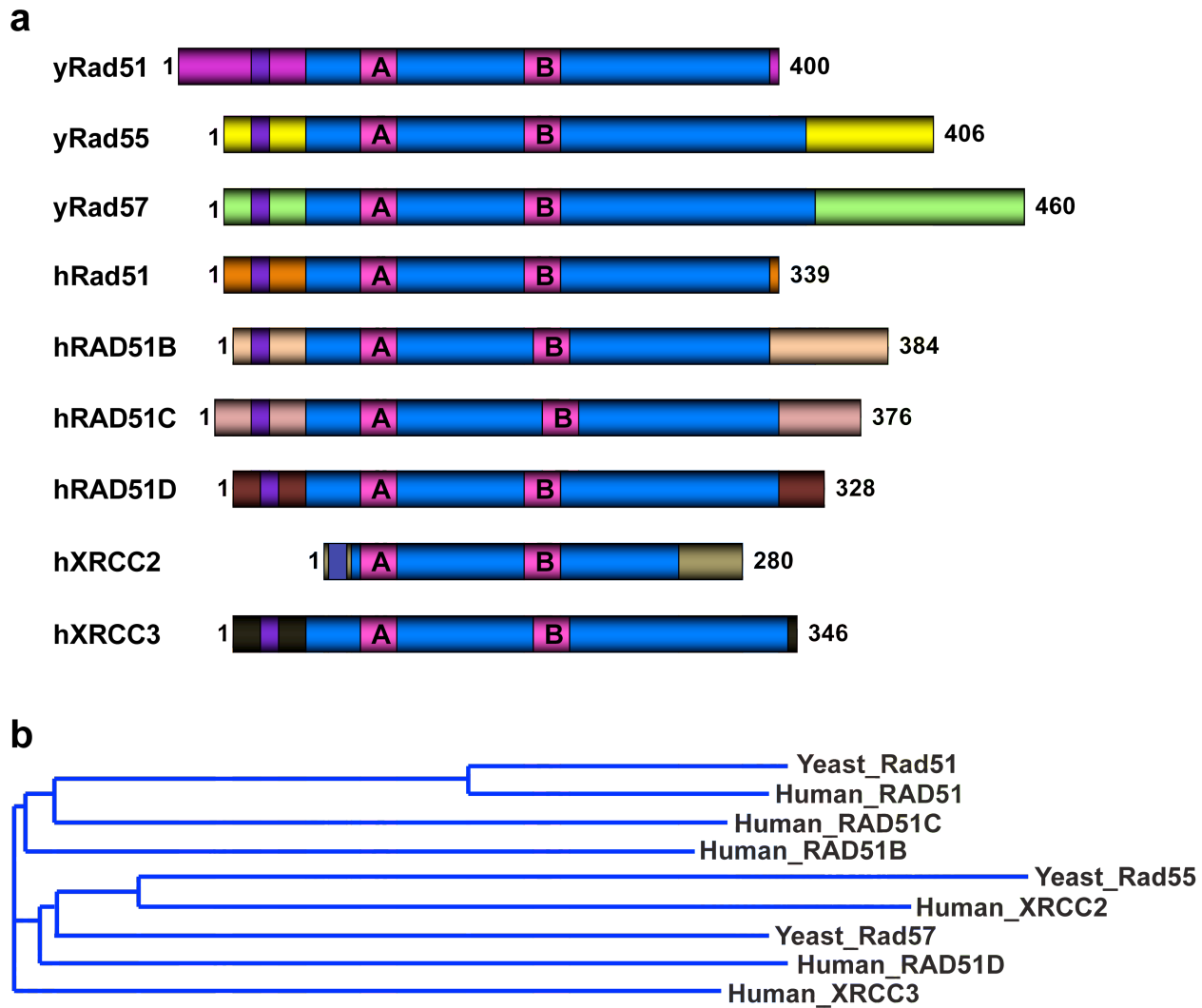
^a Strains have the common genotype *MATa leu2-3,112 trp1-289 ura3-52 his7-2 lys1-1*.

^b Strains are derivatives of W303 with the common genotype *MATa ade2-1 can1-100 his3-11,15 leu2-3,112 trp1-1 ura3-1 RAD5*. *URA3^{Kl}* denotes the *URA3* gene from *Kluveromyces lactis*.



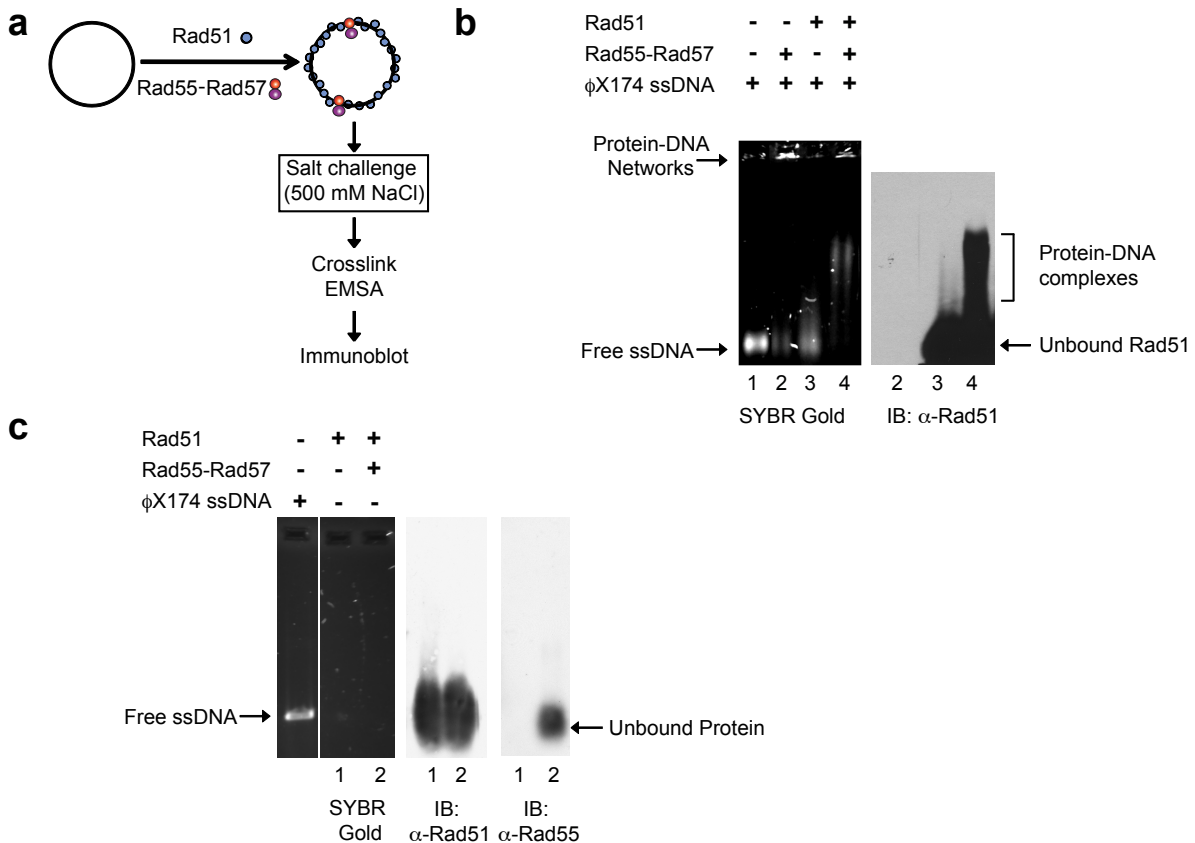
Supplementary Figure 1. Model for Rad55-Rad57 function to balance Rad51-ssDNA filament assembly and disassembly and potential influence of post-translational

modifications. **a**, Left, DSBs can be generated by cellular processes (*e.g.* endonucleases, transposases, reactive oxygen species, broken/collapsed replication forks) or by extrinsic means (*e.g.* ionizing radiation). After resection, 3'-OH ending ssDNA tails are bound by ssDNA binding protein RPA (not shown for simplicity). Rad51 protein nucleates small filament clusters that are sensitive to dissociation by Srs2 anti-recombinase. The presence of Rad55-Rad57 stabilizes Rad51 filaments and allows recombinational repair of DSBs as opposed to alternative pathways such as NHEJ or SSA¹. Right, ssDNA gaps occur in the wake of replication fork stalling (the blocking lesion is indicated). Rad51 forms small filament clusters on the ssDNA (RPA not shown) that are sensitive to Srs2 dissociation. From genetic experiments it has been inferred that spontaneous recombination in yeast is initiated rather at ssDNA gaps than at DSBs^{2,3} and that Rad55-Rad57 are particularly required for gap repair by homologous recombination instead of gap filling by TLS⁴⁻⁶. For convenience, only model 2 of the three dispositions of Rad55-Rad57 in the Rad51 filament (Figure 1e) is shown. **b**, Potential effect of post-translational modifications on pathway choice in DSB and gap repair. Post-translational modifications on Rad55-Rad57⁷, Srs2⁸, and potentially other targets¹ (see for example human RAD51⁹) controlled by the DNA damage response network (DDR) and cyclin-dependent kinases (CDK) could influence the balance between the pro-recombination activity of Rad55-Rad57 and the anti-recombination activity of Srs2 depending on cell cycle phase (G1 versus S/G2) or genotoxic stress conditions. PCNA ubiquitylation favors recruitment of TLS polymerases, whereas PCNA sumoylation recruits Srs2¹⁰⁻¹². The enhanced requirement for Rad55-Rad57 in gap repair *versus* DSB repair could be a reflection of the presence of SUMO-PCNA, presumably leading to higher local Srs2 concentrations at stalled forks and their associated gaps.

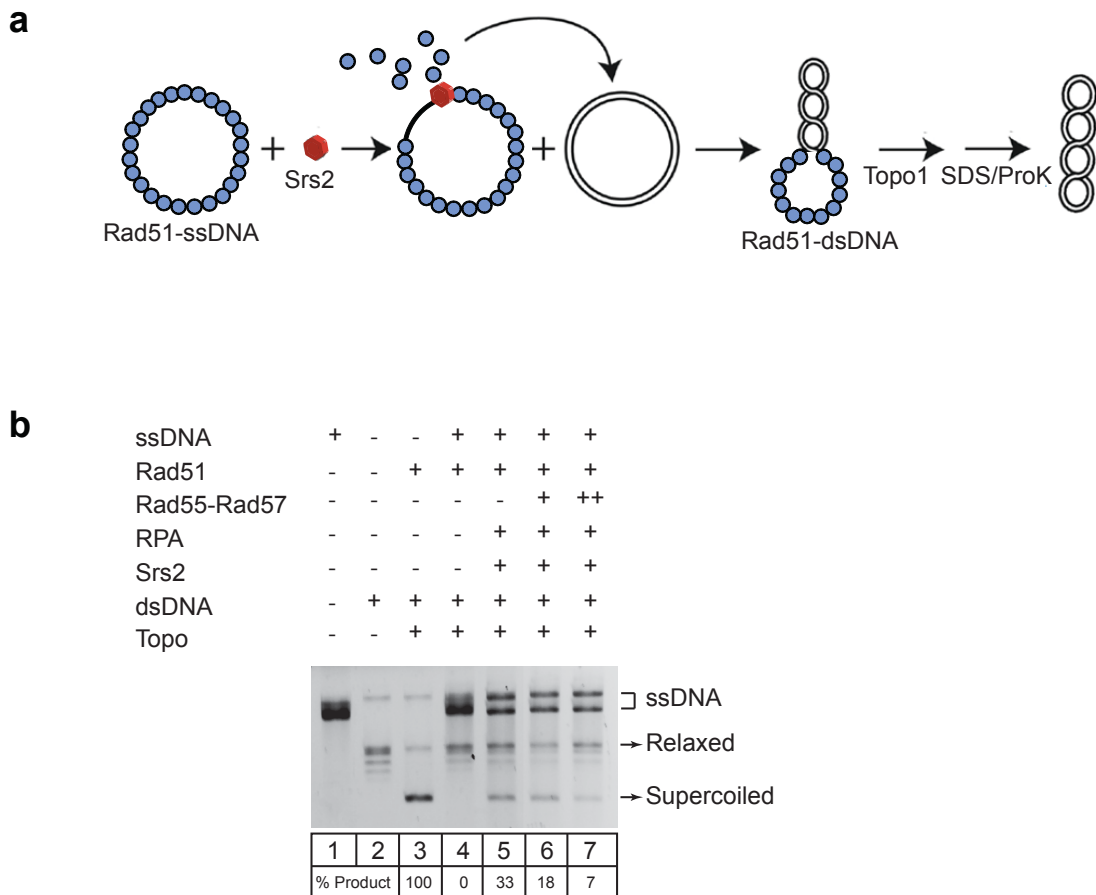


Supplementary Figure 2. Sequence conservation of Rad51 paralogs in budding yeast *S. cerevisiae* and humans.

a, Schematic representation of protein structure and sequence conservation among Rad51 paralogs, based on multiple sequence alignment of yRad51 (y=yeast), yRad55, yRad57, hRAD51 (h=human), hRAD51B, hRAD51C, hRAD51D, hXRCC2, and hXRCC3 proteins. The RecA/Rad51 core is shown in blue, and the Walker nucleotide-binding motifs are indicated as A and B. **b**, A rooted phylogram tree generated by CLUSTAL multiple sequence alignment program, showing the divergence of all paralogs listed.

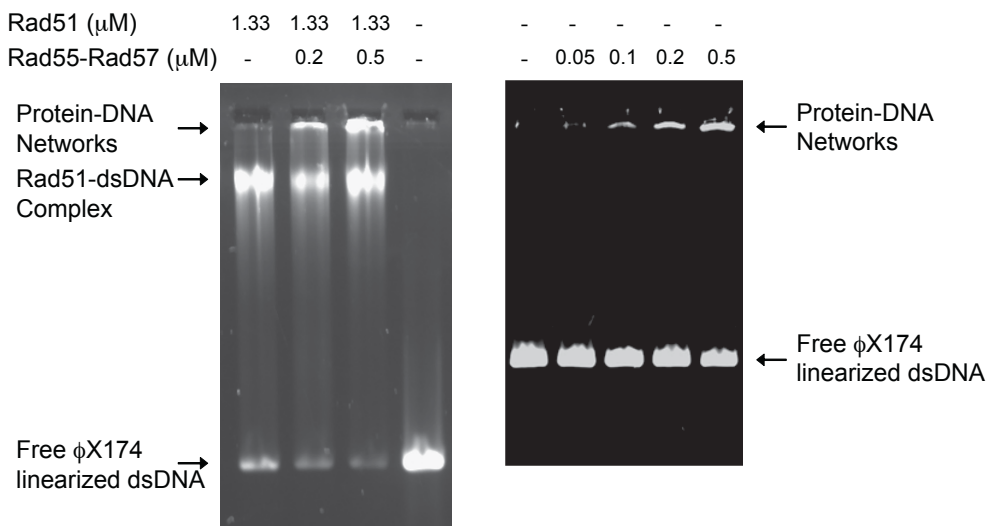


Supplementary Figure 3. Rad55-Rad57 stabilize the Rad51-ssDNA filament. **a**, Reaction scheme of Rad51-ssDNA filament salt challenge assay. For convenience, only model 2 of the three dispositions of Rad55-Rad57 in the Rad51 filament (Figure 1e) is shown. **b**, Pre-formed Rad51-ssDNA complexes (0.267 μ M 1:15 Rad51/nt) +/- Rad55-Rad57 (0.067 μ M) were challenged with 500 mM NaCl, crosslinked, and separated on an agarose gel. The presence of Rad51 in the high-salt-resistant, super-shifted protein-DNA species was confirmed by both EMSA (b, left) and immunoblot (b, right). Under these conditions, the anti-Rad55 antibodies are very inefficient in immunoblotting. **c**, Unbound protein control. 4 μ M ssDNA (in nucleotides), 0.267 μ M Rad51, or 0.267 μ M Rad51 with 0.067 μ M Rad55-Rad57 were incubated, crosslinked, and separated through electrophoresis. The migration position of the free DNA and protein species were confirmed by staining (left) and immunoblots (middle and right).

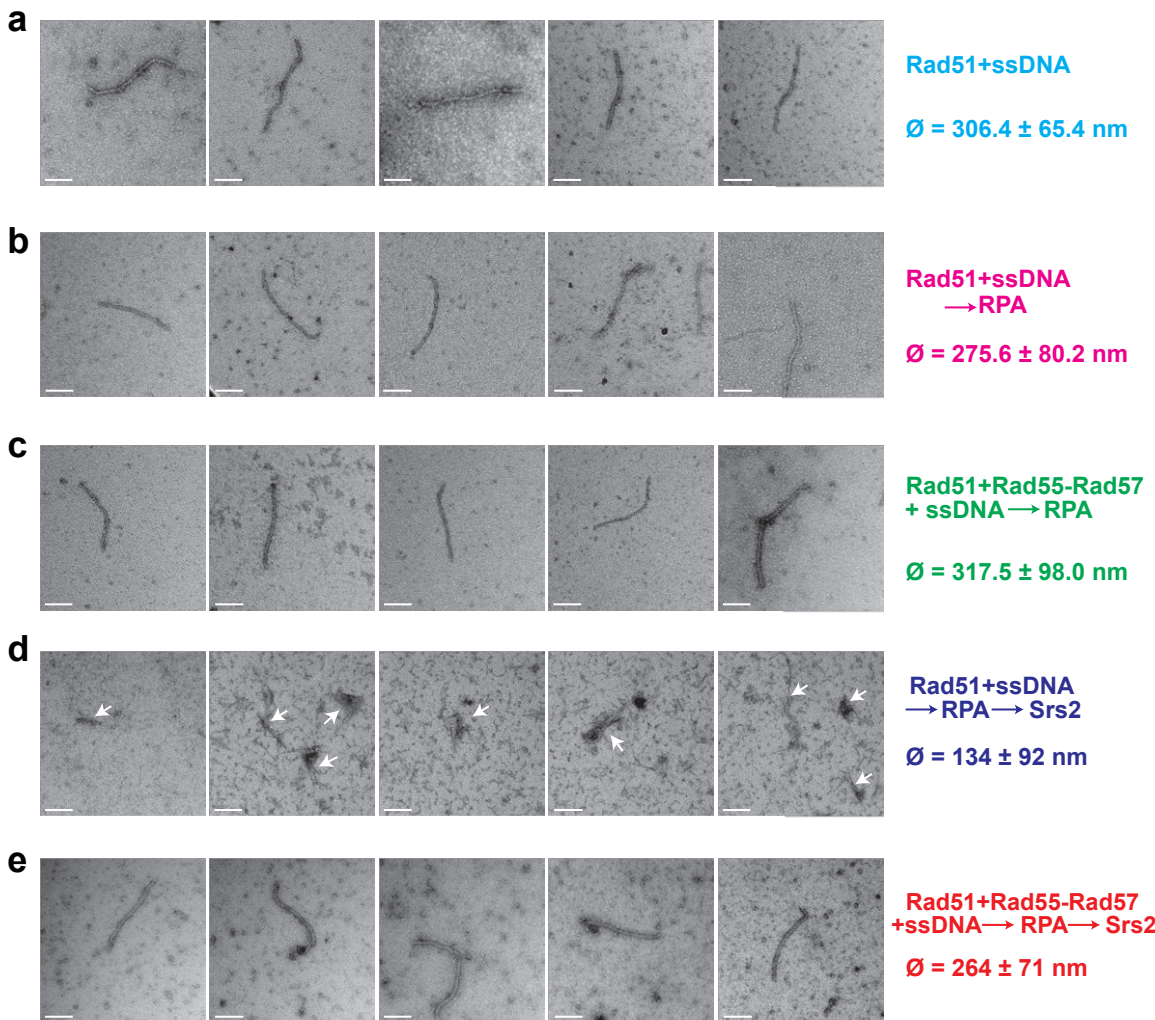


Supplementary Figure 4: Rad55-Rad57 antagonize the Srs2-catalyzed displacement of Rad51 from ssDNA in a topology-based assay. **a**, Scheme of topoisomerase I-linked DNA topology modification assay. Pre-assembled Rad51-ssDNA filaments, with or without Rad55-Rad57, are incubated with both Srs2 and RPA. Later, topologically relaxed dsDNA sharing no sequence homology was added to trap displaced Rad51 molecules from ssDNA. The reduction of DNA linking number after DNA topoisomerase I treatment reflects the extent or length of Rad51-dsDNA filament formation. Topo I: topoisomerase I. ProK: proteinase K. **b**, As indicated, 375 nM Rad51, with 0, 80, and 120 nM Rad55-Rad57, were incubated with 9 μM (in nucleotides) circular M13mp18 ssDNA for 10 min at 30 °C. Then 100 nM Srs2 and 150 nM RPA were added and incubated for 10 min, before the addition of topologically relaxed pUC19

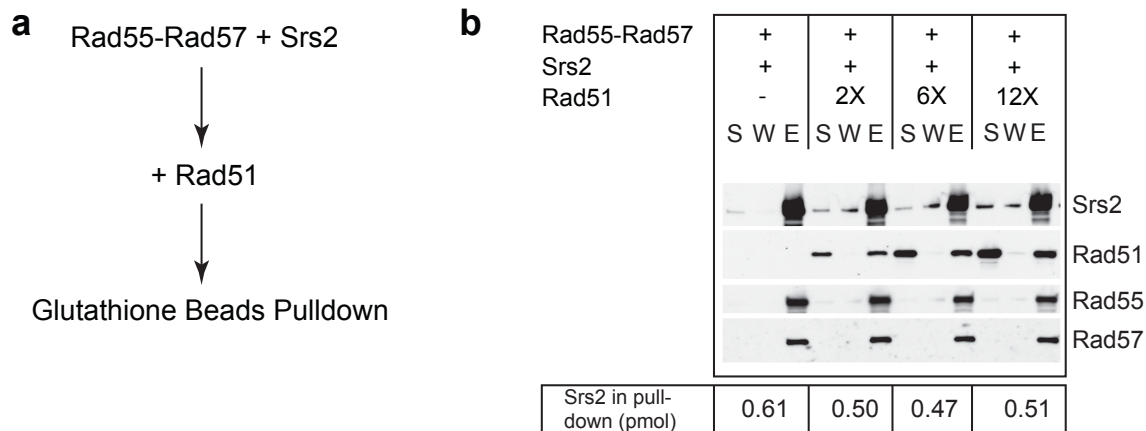
dsDNA (7 μ M in bp) and wheat germ DNA topoisomerase I (3 units). DNA species were separated on a 1 % TBE-agarose gel, stained by ethidium bromide, and quantified using ImageQuant software. The percent yield of supercoiled DNA products were calculated as a percentage of the amount of the supercoiled DNA in the control reaction condition with only Rad51 and dsDNA (lane 3)¹³. The values are the average of two independent repeats. Inhibition of Srs2-catalyzed displacement of Rad51 from ssDNA in this assay is also seen with sub-stoichiometric amounts of Rad55-Rad57 to Srs2 (data not shown) excluding the possibility that Rad55-Rad57 binds Srs2 in solution to inhibit its activity (see also Fig. 4e-g, where substoichiometric amounts of Rad55-Rad57 inhibit Srs2 translocation on ssDNA). Importantly, Rad55-Rad57 did not inhibit binding of Rad51 to dsDNA, which could potentially interfere with the interpretation of the assay (Suppl. Fig. 5).



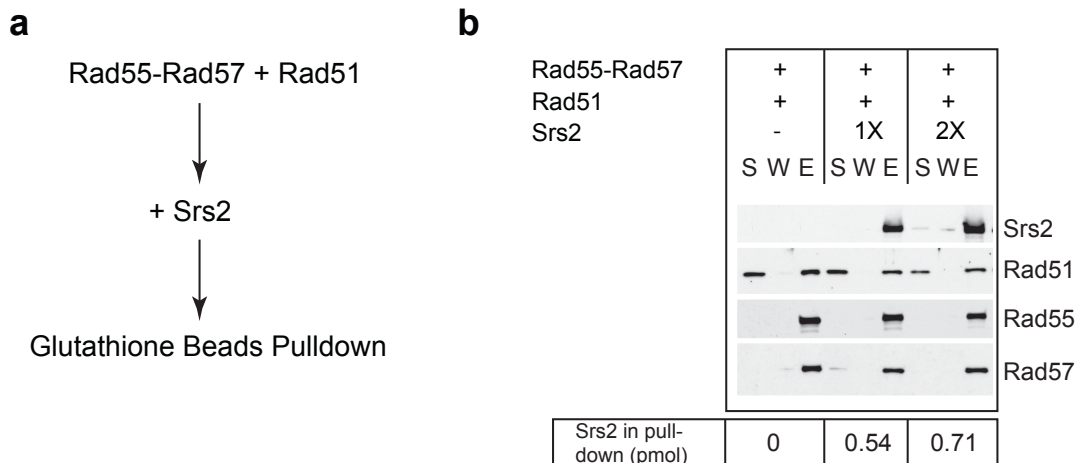
Supplementary Figure 5: Rad55-Rad57 does not inhibit Rad51 binding to dsDNA. dsDNA binding of Rad51 or Rad55-Rad57 monitored by electrophoretic mobility shift assay. Left, 1.33 μ M Rad51 was incubated with 8 μ M *Pst*I-linearized ϕ X174 dsDNA, with or without indicated amount of Rad55-Rad57. Right, indicated amount of Rad55-Rad57 was incubated with 8 μ M *Pst*I-linearized ϕ X174 dsDNA. The buffer contains 20 mM triethanolamine pH 7.5, 150 mM NaCl, 4 mM Mg(OAc)₂, 2.5 mM ATP, 25 μ g/mL BSA, 1mM DTT.



Supplementary Figure 6: EM image gallery of Rad51 filaments. **a**, Rad51 ssDNA filaments. **b**, Rad51 ssDNA filaments in the presence of RPA. **c**, Co-filaments of Rad51-Rad55-Rad57 on ssDNA in the presence of RPA. **d**, Disrupted Rad51-ssDNA filaments in the presence of Srs2 and RPA. White arrows point to ssDNA-RPA complexes. **e**, Rad51 filaments formed in the presence of Rad55-Rad57, Srs2, and RPA. The reaction conditions were the same as for Figure 2. Scale bar: 100 nm. \emptyset : mean length of Rad51 filaments.



Supplementary Figure 7: Excess Rad51 does not displace the interaction between Srs2 and Rad55-Rad57. **a**, Scheme of protein pulldown sequence. **b**, 4 nM GST-tagged Rad55-Rad57 was incubated with 8 nM Srs2 for 0.5 hr before the addition of 0, 8, 24, 48 nM Rad51 protein. After another 0.5 hr, glutathione-sepharose 4B beads were added and incubated for another hour to pull down Rad55-Rad57. 1/16th of the supernatant and wash were loaded for quantitation purpose. S: supernatant, W: wash, E: eluate.



Supplementary Figure 8: Srs2 associates with Rad55-Rad57 when pre-assembled Rad55-Rad57-Rad51 protein complexes are incubated with Srs2. **a**, Scheme of protein pulldown sequence. **b**, 4 nM GST-tagged Rad55-Rad57 was incubated with 8 nM Rad51 for 0.5 hr before the addition of 0, 4, 8 nM Srs2 protein. After another 0.5 hr, glutathione-sepharose 4B beads were added and incubated for another hour to pull down Rad55-Rad57. 1/16th of the supernatant and wash were loaded for quantitation purpose. S: supernatant, W: wash, E: eluate.

Experimental Conditions			Individual Interaction Stoichiometries		
Rad51	Rad55-Rad57	Srs2	Rad51 - Rad55-Rad57		
10	1	2	1	1	
			Srs2 - Rad55-Rad57		
			1	1	
			Rad51 - Srs2		
			1	1	

Potential Models

Model 1

1:1:1 complexes

A) Rad51 - Rad55-Rad57 - Srs2
Srs2 bound to Rad55

B) Srs2 - Rad51 - Rad55-Rad57
Srs2 bound to Rad51

Model 2

Separate 1:1 complexes

Rad51 - Rad55-Rad57
+
Rad55-Rad57 - Srs2

Model 3

Double Srs2 complex

Rad51 - Srs2
||
Rad55-Rad57 - Srs2

Model Predictions

Equal molar of Srs2, Rad51, and Rad55-Rad57 in pulldowns.

Prediction confirmed.

With ten-fold Rad51, Srs2 amount in pulldown should be down two fold. Similar binding affinity of Rad51 - Rad55-Rad57 and Srs2 - Rad55-Rad57.
Both predictions not confirmed.

Equal molar of Rad51 and Rad55-Rad57 in pulldown, but double amount of Srs2.

Prediction not confirmed.

Experimental Results

Rad51 Rad55-Rad57 Srs2
1 1 1

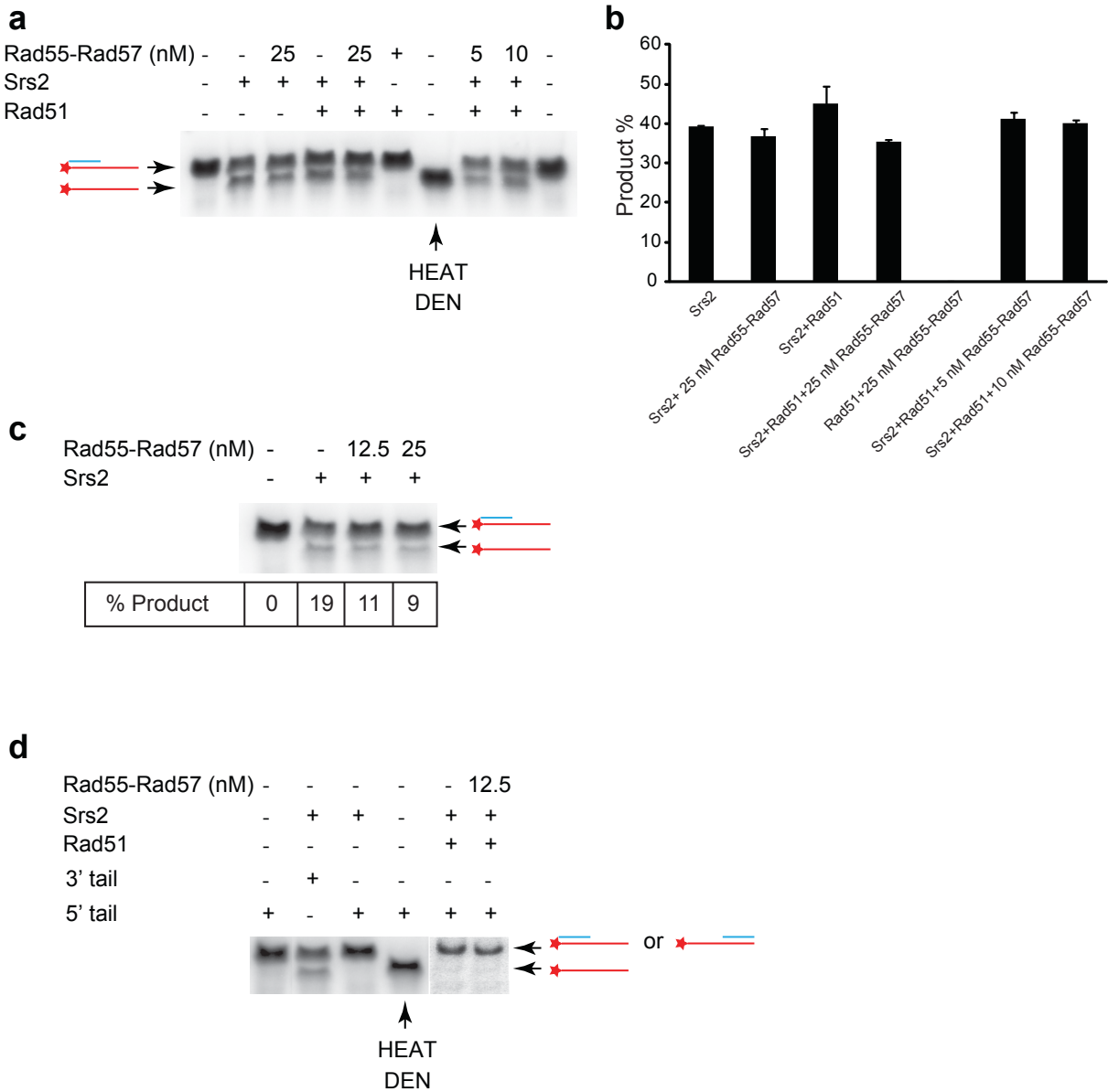
Binding Affinity

Srs2 - Rad55-Rad57
>
Rad51 - Rad55-Rad57
>
Srs2 - Rad51

Favored Model 1A over B because high affinity of Rad55-Rad57-Srs2 interaction.

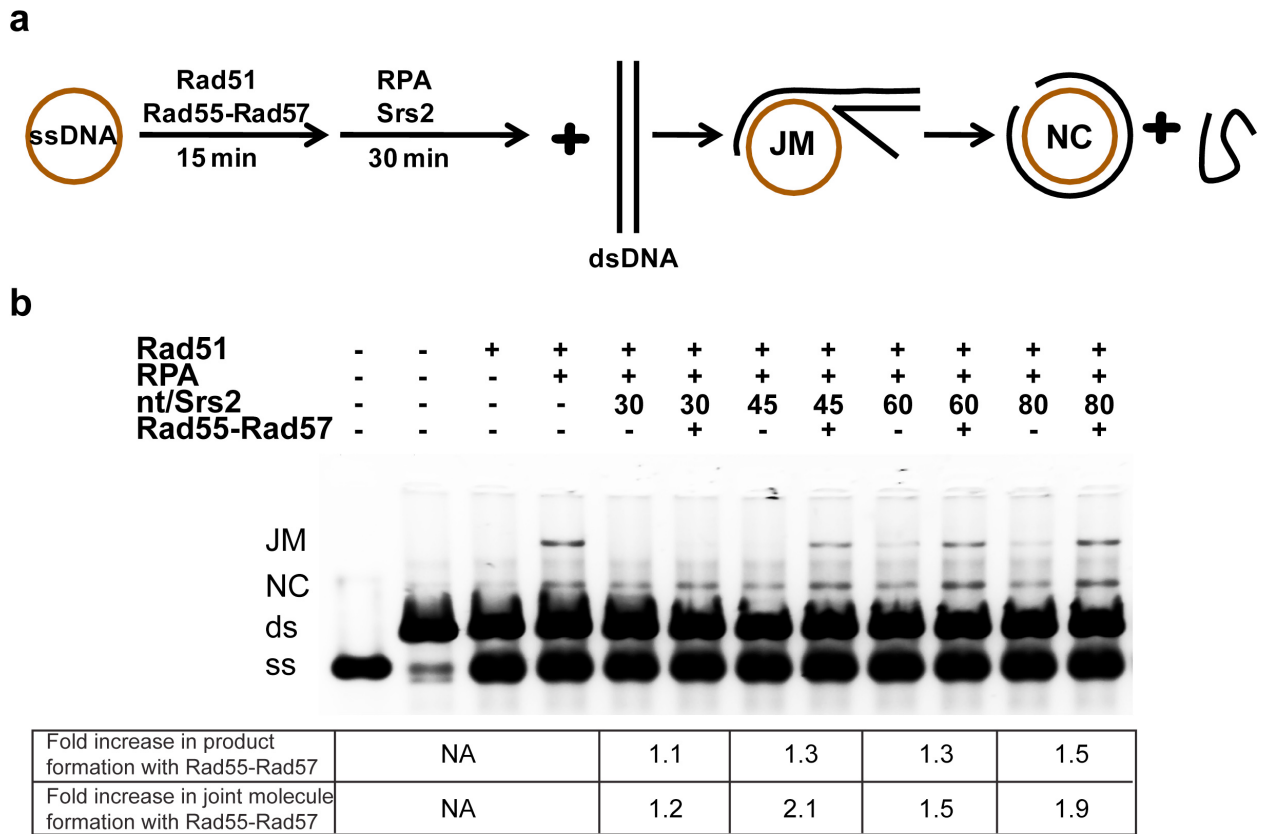
Supplementary Figure 9: Schematic representation of protein-interaction models involving

Rad51, Rad55-Rad57 and Srs2, and their experimental predictions.



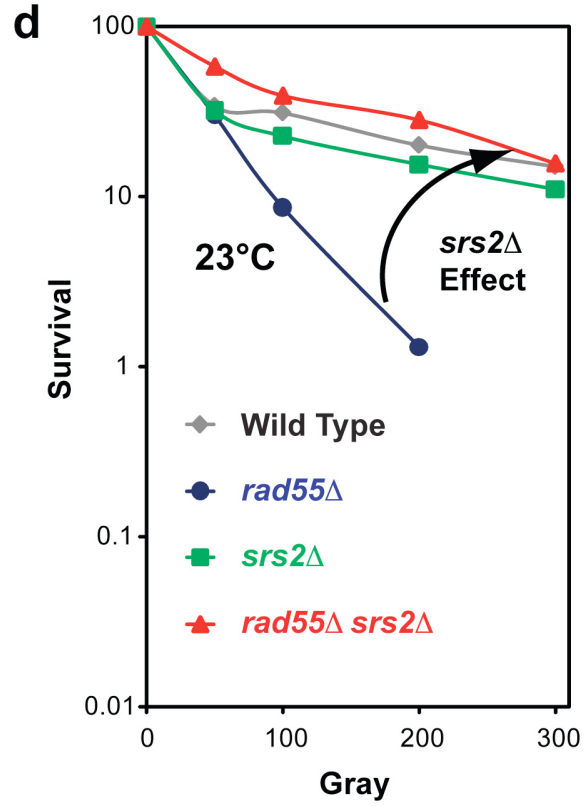
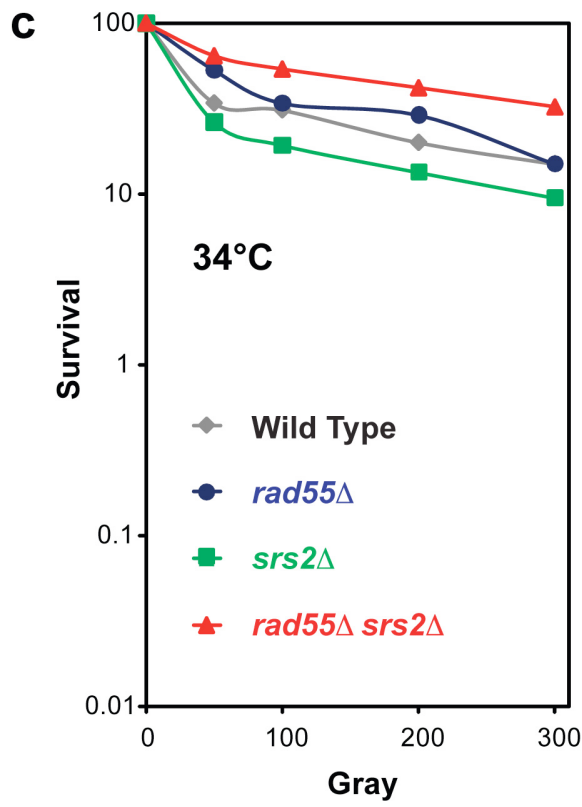
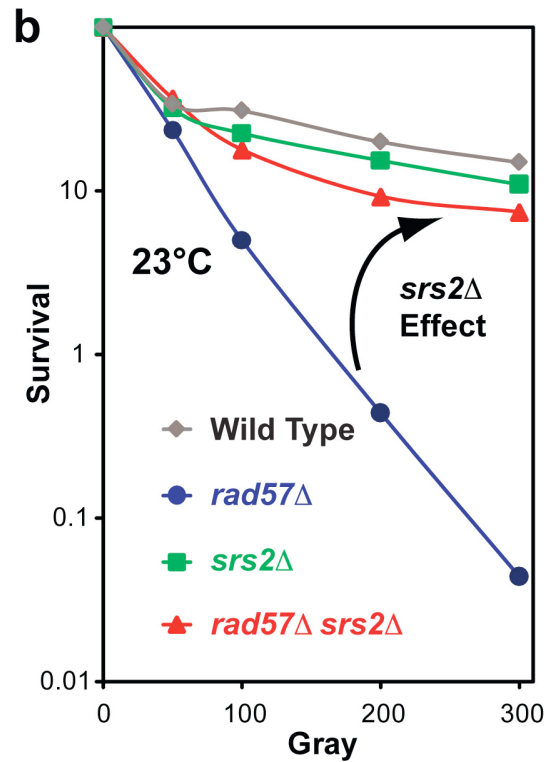
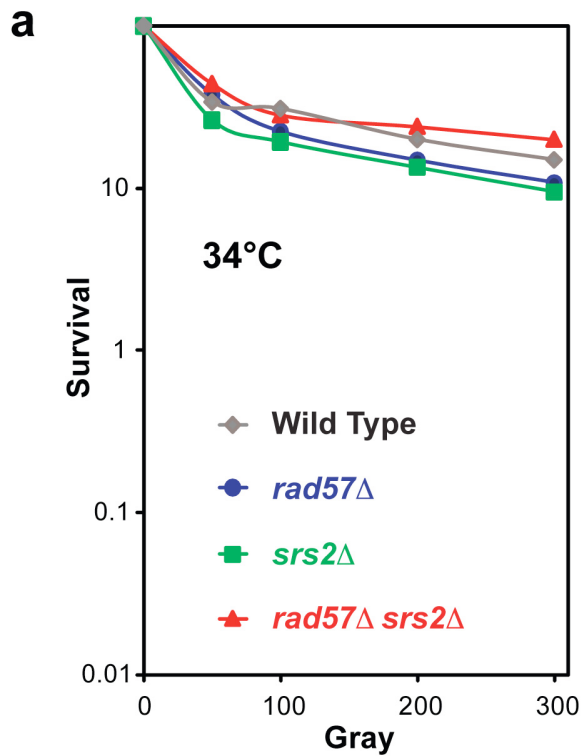
Supplementary Figure 10: Helicase control experiments. **a**, Srs2 helicase is more active under low-salt conditions. 28 nM Rad51 with indicated amount of Rad55-Rad57 were incubated with 1.5 nM oligo substrate with 3' tail for 10 min at 30 °C before the addition of 120 nM Srs2 protein to initiate helicase reaction. After 20 min incubation, the reactions were stopped and the product yields were quantified as shown in b. These reactions were performed in low salt buffer (10 mM NaCl), which allows for higher Srs2 helicase activity than under medium-salt conditions

(40 mM NaCl) in Figure 4f, g. The Rad51 stimulation of Srs2 helicase is more evident under medium-salt conditions. **c**, Rad55-Rad57 slightly inhibits the helicase activity of Srs2 in the absence of Rad51. Rad55-Rad57 was incubated with 1.5 nM oligo substrate for 10 min at 30 °C before the addition of 120 nM Srs2 protein to initiate helicase reaction. **d**, Srs2 translocates with a 3'-5' directionality. Srs2 directionality assay with 1.5 nM oligonucleotide substrate with either 3' tail or 5' tail incubated with 120 nM Srs2 for 20 min. HEAT DEN: heat denatured substrate. Reaction in c and d were performed in medium-salt conditions to serve as controls for Figure 4f, g.

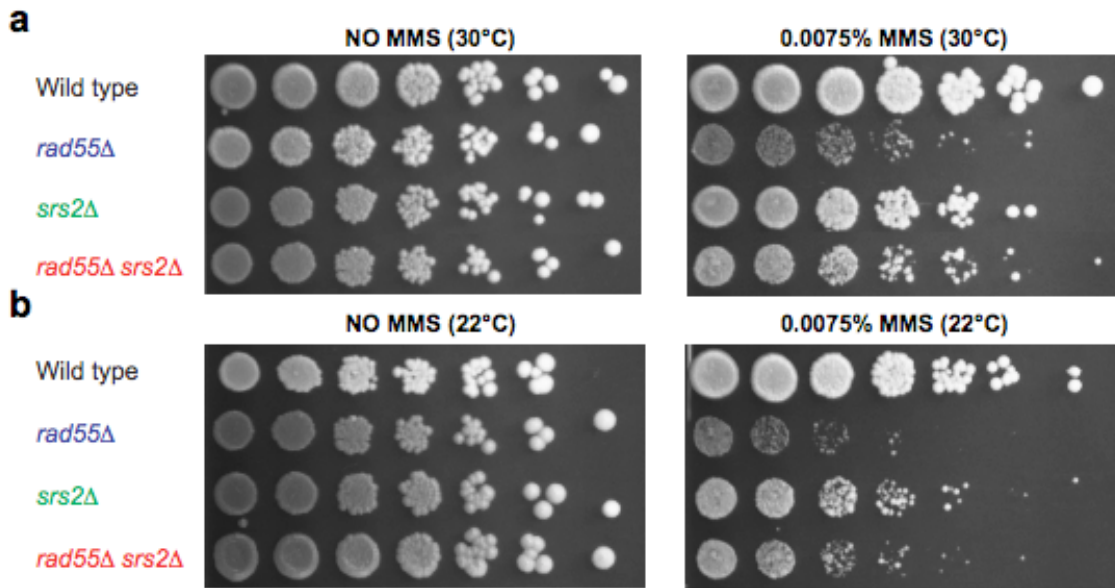


Supplementary Figure 11: Rad55-Rad57 mildly rescues Rad51-dependent strand exchange in the presence of Srs2. **a**, Reaction scheme of Rad51 DNA strand exchange in the presence of Srs2 and Rad55-Rad57. **b**, Comparison of the overall product formation and joint molecule formation in the presence and absence of Rad55-Rad57. 3.3 μM Rad51, with 0.3 μM Rad55-Rad57 or corresponding amount of Rad55-Rad57 storage buffer, was incubated with 10 μM φX174 ssDNA for 15 minutes at 30 °C. 0.56 μM RPA and 0, 333, 222, 167, 125 nM of Srs2 were added, and incubated for another 30 min. Then 10 μM (bp) PstI-linearized φX174 dsDNA and 4.8 mM spermidine were added and further incubated for 120 minutes. Percentage of product formation was calculated according to the equation product%=(JM/1.5+NC)/(JM/1.5+NC+ dsDNA). Percentage of joint molecule (JM) was calculated according to the equation JM%=(JM/1.5)/(JM/1.5+NC+dsDNA). The fold increases

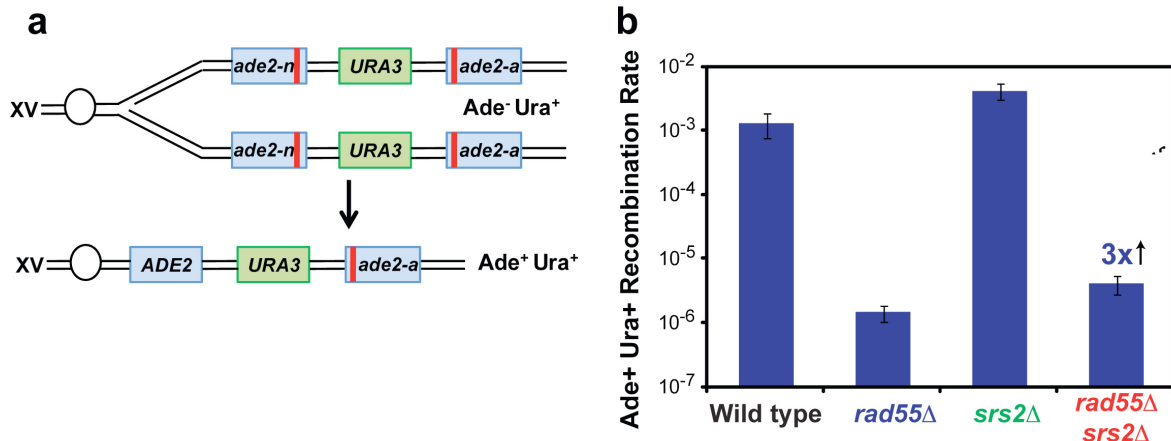
of percentages of either overall product or joint molecule formation of reactions in the presence of Rad55-Rad57 over those in the absence of Rad55-Rad57 were listed in the table below. The limited effects seen in this assay are likely a reflection of multiple roles of Srs2 (anti-recombinase¹⁴⁻¹⁹ and pro-recombination functions²⁰⁻²²).



Supplementary Figure 12. Deletion of *SRS2* suppresses the requirement for Rad55-Rad57 in DNA repair of IR-induced DNA damage. **a**, Ionizing radiation survival of wild type (FF18733), *rad57Δ* (WDHY1163), *srs2Δ* (FF18744), and *rad57Δ srs2Δ* (FF181477) at 34°C and **b**, at 23°C. **c**, Ionizing radiation survival of wild type (FF18733), *rad55Δ* (FF181461), *srs2Δ* (FF18744), and *rad55Δ srs2Δ* (FF181464) at 34°C and **d**, at 23°C. The wild type data are from ref. ²³ and additional experiments conducted at 30°C. There is no temperature effect on IR-sensitivity in wild type cells (FF, unpublished data).



Supplementary Figure 13: Deletion of *SRS2* modestly suppresses the requirement for Rad55-Rad57 in repair of MMS-induced DNA damage. **a**, MMS sensitivities of wild type (WDHY1636), *rad55Δ* (WDHY2009), *srs2Δ* (WDHY2388), and *rad55Δ srs2Δ* (WDHY2608) at 30°C and **b**, at 22°C.



Supplementary Figure 14: Deletion of *SRS2* partially suppresses the requirement for Rad55-Rad57 in mitotic recombination. **a**, Direct repeat recombination substrate and product. The substrate contains two different *ade2* alleles separated by plasmid sequences and the *URA3* gene. Both unequal sister chromatid and intrachromatid recombination between the two *ade2* repeats could generate *Ade⁺ Ura⁺* recombinants retaining the gene duplication. **b**, Rates of *Ade⁺ Ura⁺* spontaneous sister chromatid recombinants events for wild type (WDHY2319), *rad55* Δ (WDHY2019), *srs2* Δ (WDHY2632), and *rad55* Δ *srs2* Δ (WDHY2629) strains at 30°C. The 3-fold difference between the *rad55* Δ and *rad55* Δ *srs2* Δ strains is statistically significant ($p=0.021$), as determined by a student t-test.

Supplementary References

- 1 Heyer, W. D., Ehmsen, K. T. & Liu, J. Regulation of homologous recombination in eukaryotes. *Annu Rev Genet* **44**, 113-139 (2010).
- 2 Fabre, F., Chan, A., Heyer, W. D. & Gangloff, S. Alternate pathways involving Sgs1/Top3, Mus81/Mms4, and Srs2 prevent formation of toxic recombination intermediates from single-stranded gaps created by DNA replication. *Proc. Natl. Acad. Sci. USA* **99**, 16887-16892 (2002).
- 3 Lettier, G. et al. The role of DNA double-strand breaks in spontaneous homologous recombination in *S. cerevisiae*. *Plos Genetics* **2**, 1773-1786 (2006).
- 4 Fung, C. W., Mozlin, A. M. & Symington, L. S. Suppression of the Double-Strand-Break-Repair defect of the *Saccharomyces cerevisiae rad57* mutant. *Genetics* **181**, 1195-1206 (2009).
- 5 Mozlin, A. M., Fung, C. W. & Symington, L. S. Role of the *Saccharomyces cerevisiae Rad51* Paralogs in Sister Chromatid Recombination. *Genetics* **178**, 113-126 (2008).
- 6 Fung, C. W., Fortin, G. S., Peterson, S. E. & Symington, L. S. The *rad51-K191R* ATPase-defective mutant is impaired for presynaptic filament formation. *Mol. Cell. Biol.* **26**, 9544-9554 (2006).
- 7 Herzberg, K. et al. Phosphorylation of Rad55 on serines 2, 8, and 14 is required for efficient homologous recombination in the recovery of stalled replication forks. *Mol. Cell. Biol.* **26**, 8396-8409 (2006).
- 8 Saponaro, M. et al. Cdk1 Targets Srs2 to Complete Synthesis-Dependent Strand Annealing and to Promote Recombinational Repair. *Plos Genetics* **6**, e1000858 (2010).
- 9 Sorensen, C. S. et al. The cell-cycle checkpoint kinase Chk1 is required for mammalian homologous recombination repair. *Nat. Cell Biol.* **7**, 195-201 (2005).
- 10 Pfander, B., Moldovan, G. L., Sacher, M., Hoege, C. & Jentsch, S. SUMO-modified PCNA recruits Srs2 to prevent recombination during S phase. *Nature* **436**, 428-433 (2005).
- 11 Papouli, E. et al. Crosstalk between SUMO and ubiquitin on PCNA is mediated by recruitment of the helicase Srs2p. *Mol. Cell* **19**, 123-133 (2005).
- 12 Burgess, R. C. et al. Localization of recombination proteins and Srs2 reveals anti-recombinase function in vivo. *J. Cell Biol.* **185**, 969-981 (2009).
- 13 Schwendener, S. et al. Physical interaction of RECQL helicase with RAD51 facilitates its anti-recombinase activity. *J Biol Chem* **285**, 15739-15745 (2010).
- 14 Schiestl, R. H., Prakash, S. & Prakash, L. The *SRS2* suppressor of *rad6* mutations of *Saccharomyces cerevisiae* acts by channeling DNA lesions into the *RAD52* DNA repair pathway. *Genetics* **124**, 817-831 (1990).
- 15 Aboussekhra, A. et al. *RADH*, a gene of *Saccharomyces cerevisiae* encoding a putative DNA helicase involved in DNA repair. Characteristics of *radH* mutants and sequence of the gene. *Nucleic Acids Res.* **17**, 7211-7219 (1989).
- 16 Aguilera, A. & Klein, H. L. Genetic control of intrachromosomal recombination in *Saccharomyces cerevisiae*. I. Isolation and genetic characterization of hyper-recombination mutations. *Genetics* **119**, 779-790 (1988).
- 17 Krejci, L. et al. DNA helicase Srs2 disrupts the Rad51 presynaptic filament. *Nature* **423**, 305-309 (2003).
- 18 Veaute, X. et al. The Srs2 helicase prevents recombination by disrupting Rad51 nucleoprotein filaments. *Nature* **423**, 309-312 (2003).
- 19 Antony, E. et al. Srs2 Disassembles Rad51 Filaments by a Protein-Protein Interaction Triggering ATP Turnover and Dissociation of Rad51 from DNA. *Mol. Cell* **35**, 105-115 (2009).
- 20 Aylon, Y., Liefshitz, B., Bitan-Banin, G. & Kupiec, M. Molecular dissection of mitotic recombination in the yeast *Saccharomyces cerevisiae*. *Mol Biol Cell* **23**, 1403-1417 (2003).

- 21 Ira, G., Malkova, A., Liberi, G., Foiani, M. & Haber, J. E. Srs2 and Sgs1-Top3 suppress crossovers during double-strand break repair in yeast. *Cell* **115**, 401-411 (2003).
- 22 Dupaigne, P. *et al.* The Srs2 helicase activity is stimulated by Rad51 filaments on dsDNA: Implications for crossover incidence during mitotic recombination. *Mol. Cell* **29**, 243-254 (2008).
- 23 Aboussekhra, A., Chanet, R., Adjiri, A. & Fabre, F. Semi-dominant suppressors of Srs2 helicase mutations of *Saccharomyces cerevisiae* map in the *RAD51* gene, whose sequence predicts a protein with similarities to prokaryotic RecA protein. *Mol. Cell. Biol.* **12**, 3224-3234 (1992).